

# Large Protein Assemblies for High-Relaxivity Contrast Agents: The Case of Gadolinium-Labeled Asparaginase

Giulia Licciardi, Domenico Rizzo, Maria Salobehaj, Lara Massai, Andrea Geri, Luigi Messori, Enrico Ravera, Marco Fragai, and Giacomo Parigi\*



Cite This: *Bioconjugate Chem.* 2022, 33, 2411–2419



Read Online

ACCESS |



Metrics & More

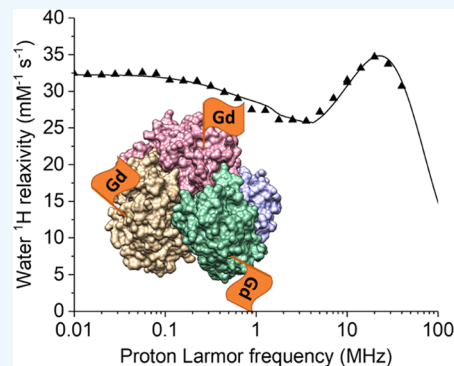


Article Recommendations



Supporting Information

**ABSTRACT:** Biologics are emerging as the most important class of drugs and are used to treat a large variety of pathologies. Most of biologics are proteins administered in large amounts, either by intramuscular injection or by intravenous infusion. Asparaginase is a large tetrameric protein assembly, currently used against acute lymphoblastic leukemia. Here, a gadolinium(III)-DOTA derivative has been conjugated to asparaginase, and its relaxation properties have been investigated to assess its efficiency as a possible theranostic agent. The field-dependent  $^1\text{H}$  longitudinal relaxation measurements of water solutions of gadolinium(III)-labeled asparaginase indicate a very large increase in the relaxivity of this paramagnetic protein complex with respect to small gadolinium chelates, opening up the possibility of its use as an MRI contrast agent.



## INTRODUCTION

The millions of MRI exams performed annually in the world after administration of gadolinium(III) contrast agents and the concerns about their safety continuously stimulate the efforts for the development of safer contrast agents.<sup>1</sup> The contrast agents used in the clinics are nowadays almost exclusively small gadolinium(III) complexes. Administration of these complexes has been shown to determine gadolinium accumulation in the tissues of the patients, thus raising concerns for their long-term consequences on health.<sup>2,3</sup> For instance, they have been associated with nephrogenic systemic fibrosis in patients with impaired renal clearance.<sup>4–6</sup>

The strategy to reduce the risks associated with the administration of contrast agents without reducing the quality, and thus the diagnostic accuracy, of the MRI images, passes through the use of molecules not containing gadolinium(III) ions but similarly able to enhance the nuclear relaxation rates of water protons,<sup>7–10</sup> or through the development of gadolinium complexes with higher efficiency so that the injected dose can be sizably reduced. A reduction of the injected gadolinium(III) dose can be achieved (i) by targeting the contrast agents to specifically accumulate them in the tissues of interest and (ii) by increasing the capability of the agents to enhance the water proton relaxation rates. This capability is called relaxivity and is defined as the enhancement in the water proton relaxation rate due to a gadolinium concentration of 0.001 mol dm<sup>-3</sup>.

An effective way to increase relaxivity at low and intermediate magnetic fields (below ca. 1 T) is slowing down the reorientation mobility of the complex. This can be

achieved by functionalizing low-molecular-weight gadolinium(III) complexes to bind noncovalently to macromolecules,<sup>11–13</sup> by confining them within nanosized matrices, like nanogels,<sup>14–18</sup> or by exploiting nanosized gadolinium(III)-based compounds.<sup>19–24</sup> On the other hand, an increase in the reorientation time of the contrast agent determines a decrease in relaxivity at high magnetic fields. The optimal reorientation time  $\tau_R$  is related to the applied magnetic field  $B_0$  through the relationship  $\tau_c^{\text{opt}} = (\gamma_I B_0)^{-1}$ , with  $\tau_c^{-1} = \tau_R^{-1} + \tau_M^{-1} + R_{1e}$ , where  $\gamma_I$  is the proton magnetogyric ratio,  $\tau_M$  is the lifetime of the water molecule(s) coordinated to the gadolinium(III) ion, and  $R_{1e}$  is the electron relaxation rate.<sup>25,26</sup> At 1.5 T, if water exchange and electron relaxation are slower than molecular reorientation,  $\tau_R^{\text{opt}} = 2.5$  ns. Therefore, reorientation times in the nanosecond timescale are needed to achieve the highest relaxivities at the fields of MRI scanners.

Metalloprotein-based contrast agents have been considered because of the ease of preparation and the availability of engineering techniques that can allow for their functionalization and targeting.<sup>27</sup> The relaxivity of (either natural or metal-substituted) paramagnetic metalloproteins is however typically limited, despite their overall reorientation times of the order of nanoseconds or larger, due to the presence of paramagnetic

Received: October 28, 2022

Revised: November 22, 2022

Published: December 2, 2022



ions (different from gadolinium) with short electron relaxation times, and/or the long lifetime of coordinated water molecules. Proteins engineered by rational design were thus proposed by creating a gadolinium-binding site with strong metal selectivity in a stable and potentially fully functioning host protein.<sup>28,29</sup>

Chimeric proteins were also constructed by inserting an EF-hand motif, which can bind a gadolinium ion, into a functionalized protein.<sup>30–32</sup> However, the application of these chimeric proteins is limited by their metal binding affinities which are much weaker than those of the chelates approved for clinical use. A high binding affinity and metal selectivity was achieved by engineering an EF-hand motif of the protein  $\alpha$ -parvalbumin.<sup>33</sup>

An easier, preferable alternative is attaching a paramagnetic tag to a diamagnetic protein, like albumin and immunoglobulins.<sup>34</sup> Gadolinium(III) ions can be attached to proteins by bifunctional chelates, usually DOTA-like or DTPA-like complexes with an electrophilic group for conjugation to nucleophilic groups of macromolecules.<sup>35</sup> The possibility of genetically engineering protein polymers at multiple backbone sites allows attaching multiple paramagnetic tags per protein.<sup>36,37</sup> This results in multivalent, biomacromolecular contrast agents endowed with extremely high relaxivity per particle, although the relaxivity per gadolinium ion is often limited. GdDTPA-monoamide tethered to polylysine<sup>38</sup> or dextran,<sup>39</sup> for instance, shows low relaxivities because of the internal mobility which limits the relaxivity enhancement.<sup>40</sup> Furthermore, an increase in the water lifetime of about a factor 3 has been observed upon the replacement of one carboxylate function by an amide in both DOTA-like and DTPA-like chelates.<sup>41</sup>

Along these lines, we have attached a derivative of 1,4,7,10-tetraazacyclododecane-1,4,7,10-tetraacetic acid (DOTA) to the protein L-asparaginase II (ANSII), a biological drug in clinical use against leukemia. Together with the four macrocyclic nitrogen atoms, four acetate arms of the chelate coordinate the gadolinium(III) ion, and the carboxylate group on the 5-carbon arm, activated with the ester, is used for covalent attachment to the primary amine of lysine residues via amide bond formation (Figure 1).<sup>35</sup> Carboxylates and

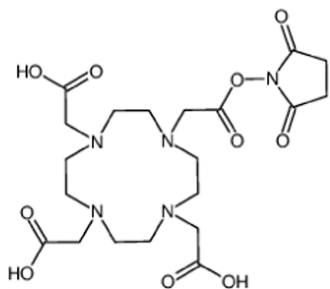


**Figure 1.** 1,4,7,10-Tetraazacyclododecane-1,4,7,10-tetraacetic acid mono-*N*-hydroxysuccinimide ester (DOTA-NHS-ester) chemical structure.

backbone carbonyls, and hydroxyls to a lesser extent, can also coordinate lanthanoids.<sup>42</sup> However, it has long been proven that in the presence of a high-affinity chelator and after thorough purification, the ions aspecifically bound to the protein surface are in negligible concentration.<sup>43,44</sup> Analogous paramagnetic tags were previously attached to dendrimers, silica nanoparticles, or proteins like albumin through

methanethiosulfonate anchor groups.<sup>45</sup> In these cases, they showed a relaxivity not exceeding  $25 \text{ s}^{-1} \text{ mM}^{-1}$  even at the peak magnetic field because of being limited by a subnanosecond reorientation time and a rather long lifetime of the coordinated water molecule.<sup>45,46</sup>

ANSII consists of four identical subunits, forming a dimer of dimers of 138 kDa with  $D_2$  symmetry, with an extensive mobility in the nanosecond timescale.<sup>47</sup> The attachment of a paramagnetic tag to ANSII is thus expected to result in an MRI contrast agent of much improved relaxivity with respect to those presently used in clinics, and of the order of that of previously reported paramagnetic proteins. Here, the relaxivity properties of the Gd(III)-DOTA-NHS-ester conjugated to amine groups of ANSII have been investigated in detail to evaluate the relaxation enhancement achieved upon conjugation. Indeed, we found a relaxivity at  $37^\circ\text{C}$  as large as ca.  $35 \text{ s}^{-1} \text{ mM}^{-1}$  at the peak magnetic field.

Most importantly, this protein represents an attractive carrier for the delivery of the paramagnetic moiety because:

- (1) ANSII is one of the oldest biologics approved for clinical use as a drug against acute lymphoblastic leukemia both in its native and PEGylated forms.<sup>48</sup> It is currently used in humans by intramuscular injection or by intravenous infusion three times weekly. The grafting of gadolinium(III) tags is not expected to affect the therapeutic efficacy of ANSII as proved by the enzymatic activity of the clinically approved highly PEGylated form of the enzyme, where most of the surface exposed lysines are conjugated to PEG chains.<sup>49</sup> Therefore, this protein is a good model to develop protein-based theranostic agents and also to develop new strategies to investigate the pharmacokinetics and fate of biologics.
- (2) Each of the four ANSII subunits contains 22 lysine residues, which can be largely functionalized.<sup>50</sup> The many solvent-exposed lysine residues can thus allow for the conjugation of a huge amount of paramagnetic chelates to the same protein. In perspective, this can allow the development of an agent carrying a high payload of paramagnetic ions.

## RESULTS AND DISCUSSION

**Preparation and Characterization of the Conjugated Protein.** The functionalization of ANSII with DOTA-NHS-ester was carried out as described in the [Experimental Procedures](#) section. Considering the lower  $pK_a$  of the  $\alpha$ -amine of the N-terminus compared to the  $\epsilon$ -amine of lysines, as a result of the inductive effects of the nearby carbonyl group, at pH 7.5, a selective acylation and alkylation of N-terminal amines is favored, although complete site specificity is not achieved.<sup>51,52</sup> Under these conditions, a few amines in the protein are expected to be significantly reactive.<sup>53,54</sup> Mild conditions for conjugation were employed, as we aimed at evaluating the paramagnetic relaxation enhancement with distant gadolinium(III) ions, to avoid possible magnetic coupling. Gadolinium(III) was added in defect, and the addition was followed by gel filtration purification. ICP-OES was employed to determine the gadolinium(III) concentration into the sample; it was found to correspond to the presence of 3 gadolinium(III) ions per tetramer.

**ESI MS Characterization of the Free and Conjugated Protein.** The free and DOTA-NHS-ester conjugated protein were further characterized through ESI MS analysis according

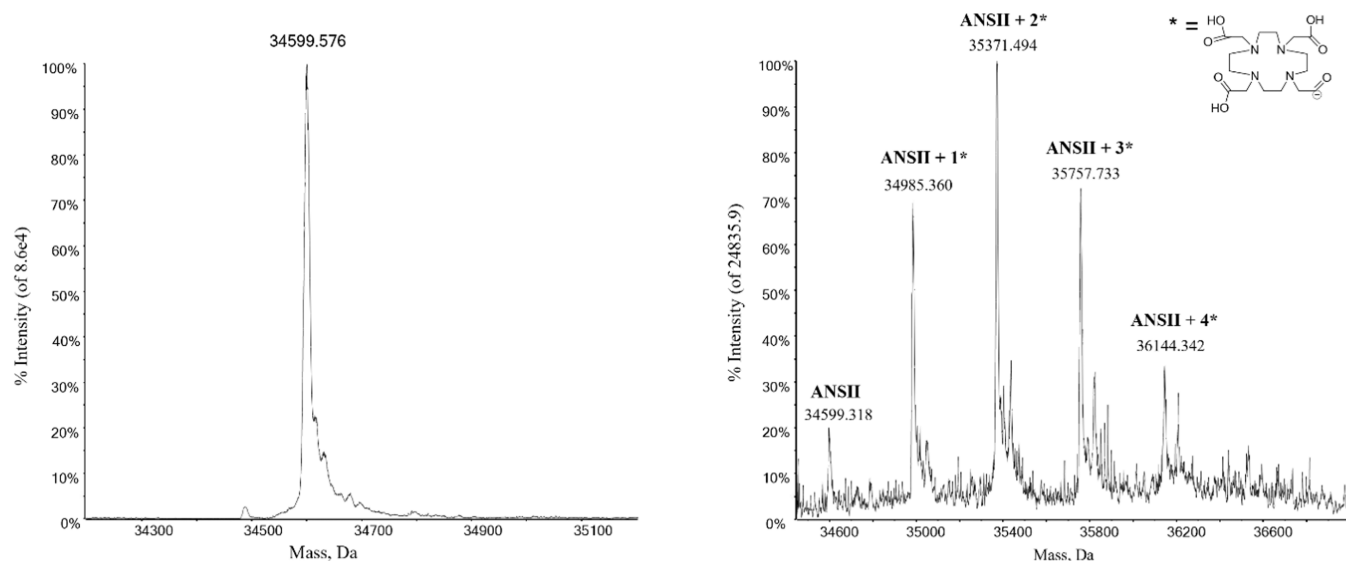


**Figure 2.** Deconvoluted mass spectra of ANSII  $10^{-6}$  M (left panel) and deconvoluted mass spectra of DOTA-NHS conjugated protein  $10^{-6}$  M (right panel).

to standard procedures.<sup>55,56</sup> The ESI MS spectrum of the free protein is shown in Figure 2a. The deconvoluted ESI MS spectrum shows an intense and very well resolved single peak with a mass of 34 599 Da. This value is very close—though not identical (there is an apparent difference of a few Daltons)—to the calculated value for the sequence of the protein reported in UNIPROT (P00805) being equal to 34 595 Da. Upon inspection of the ESI MS spectrum, it emerges that the ANSII protein shows a high degree of purity. The spectrum of the DOTA-NHS-ester conjugated protein, prepared as described in the Experimental Procedures section, is reported in Figure 2b. The latter spectrum shows a number of additional peaks with mass values greater than the free protein. Notably, the peaks at 34 985, 35 371, 35 757, and 36 144 Da are straightforwardly assigned to protein conjugates bearing one, two, three, and four DOTA-NHS-ester moieties, respectively. The percentage ratios between free ANSII and the various forms of ANSII conjugated with DOTA-NHS are reported in Figure S1. This means that the sample contains in comparable amounts a few species with a variable number of DOTA-NHS-ester groups. It is known that the DOTA-NHS-ester manifests a large selectivity for free amino groups, but it is difficult to identify by MS which lysine groups are actually modified. As only a rather limited number of lysine groups are modified even in the presence of relatively large DOTA-NHS-ester/protein ratios 15:1, it can be inferred that only the most accessible and reactive lysine groups will be modified. A plausible estimation of the most accessible and reactive lysines has been obtained independently through a bioinformatic analysis using the program PROPKA.<sup>53,54</sup> This analysis suggests that the most reactive amino groups residues are the N-terminus and lysines 104, 49, and 71 (see Table S1).

**Water  $^1\text{H}$  NMRD Profiles of ANSII-DOTA.** The  $^1\text{H}$  NMRD profiles of water solutions of diamagnetic (metal free) ANSII-DOTA at 15, 25, and 37 °C are shown in Figure 3. The concentration of the monomeric protein was  $0.38\text{ mmol dm}^{-3}$ .

The decrease in the relaxation rates measured for increasing magnetic fields reports on the dynamics of the water protons interacting with the protein.<sup>57</sup> Their dipole–dipole coupling energy is modulated by the shortest time between the overall

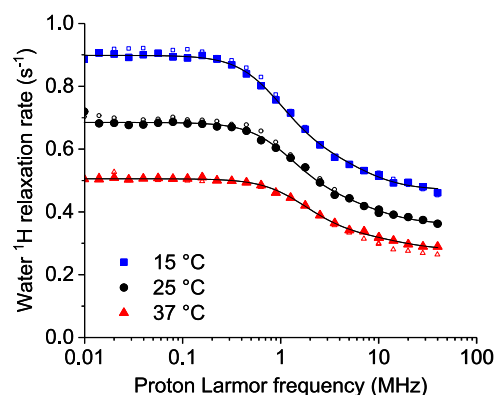


**Figure 3.**  $^1\text{H}$  NMRD profiles of a water solution of DOTA-conjugated ANSII ( $0.38\text{ mmol dm}^{-3}$  monomeric protein concentration) at 15, 25, and 37 °C (solid symbols). Basically identical profiles were measured for the unconjugated ANSII protein (empty symbols).

reorientation time  $\tau_R$  of the tetrameric protein assembly, the local internal mobility times  $\tau_\beta$  and the lifetime  $\tau_M$  of the water molecule on the protein surface. Water molecules with  $\tau_M$  longer than  $\tau_R$  or  $\tau_\beta$  thus provide information on the molecular tumbling time and on possible presence of faster internal mobility. The  $^1\text{H}$  NMRD profiles were fitted using eq 1<sup>58,59</sup>

$$R_{1\text{dia}} = \alpha + \beta \sum_n^N c_n \left( \frac{\tau_n}{1 + \omega^2 \tau_n^2} + \frac{4\tau_n}{1 + 4\omega^2 \tau_n^2} \right) \quad (1)$$

where  $c_n$  are weight coefficients summing to 1. The profiles could not be nicely fitted with  $N = 1$ , whereas fits of good quality could be obtained with  $N = 2$  (solid lines in Figure 3). The best-fit profiles are reported in Table 1, where the longest and shortest  $\tau$ 's obtained from the fit were indicated as  $\tau_R$  and  $\tau_\beta$ , respectively.<sup>60</sup> These values are in agreement with those previously obtained for the unconjugated ANSII protein in a different concentration and water buffer solution (20 mM sodium phosphate, pH 7.5, 0.02%  $\text{NaN}_3$ , 0.1  $\text{mg mL}^{-1}$  protease inhibitors (Pefabloc)), when the following values were obtained at 25 °C:  $c_1 = 0.42$ ,  $\tau_1 = 6.0 \times 10^{-8}$  s,  $\tau_2 = 9 \times$

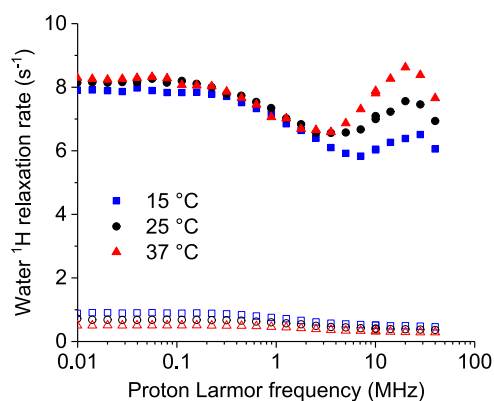
**Table 1. Best-Fit Parameters of the  $^1\text{H}$  NMRD Profiles of DOTA-Conjugated ANSII**

	15 °C	25 °C	37 °C	
$\alpha$	0.47	0.36	0.28	$\text{s}^{-1}$
$\beta$		$1.2 \times 10^7$		$\text{s}^{-2}$
$c_1$		0.31		
$\tau_R = \tau_1$	$8.7 \times 10^{-8}$	$6.7 \times 10^{-8}$	$4.9 \times 10^{-8}$	s
$\tau_t = \tau_2^a$	$1.3 \times 10^{-8}$	$9.3 \times 10^{-9}$	$5.5 \times 10^{-9}$	s

$$^a c_2 = 1 - c_1.$$

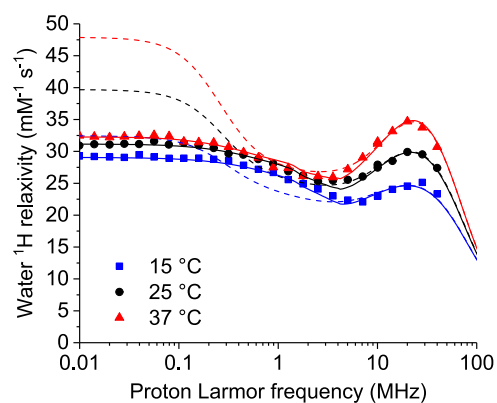
$10^{-9}$  s.<sup>50</sup> The values of  $\tau_R$  confirm that indeed the protein forms tetrameric assemblies, being of the order of what expected for globular proteins with MW of ca. 140 kDa.<sup>58</sup> This finding represents an evidence that the tetrameric structure of the unconjugated protein is retained also upon its functionalization with DOTA-NHS-ester. The large contribution from correlation times smaller than 10 ns (at 25 °C) indicate the presence of an extensive mobility in the nanosecond timescale, probably reflecting the intrinsic flexibility related to the many loop regions present in the protein. As previously noted, this extensive internal mobility is consistent with the intensity and resolution of the solution NMR spectra of the protein.<sup>50</sup>

**Water  $^1\text{H}$  NMRD Profiles of Gd-DOTA-Conjugated ANSII.** The NMRD profiles of the water solution of Gd-DOTA-conjugated ANSII were collected at 15, 25, and 37 °C (Figure 4). The concentration of the gadolinium(III) ions was

**Figure 4.**  $^1\text{H}$  NMRD profiles of a water solution of Gd-DOTA-conjugated ANSII ( $0.24 \text{ mmol dm}^{-3}$ ) at 15, 25, and 37 °C (solid symbols). The profiles of the Gd-free protein are also shown as empty symbols.

$0.24 \text{ mmol dm}^{-3}$ , as determined from ICP-OES measurements. The relaxivity values, obtained from the difference between the relaxation rates measured from the paramagnetic and the diamagnetic samples, scaled to  $1 \text{ mmol dm}^{-3}$  gadolinium(III) concentration, are shown in Figure 5.

Interestingly, the relaxivity is quite large (although much smaller than the theoretical limit<sup>61</sup>) for a complex with one water molecule ( $q = 1$ ) coordinated to the gadolinium ion, with respect to that measured for other proteins conjugated to DOTA-like or DTPA-like complexes. Nevertheless, the temperature dependence of the profiles indicates that the relaxivity is limited by the water protons exchange rate, as it increases with the temperature. The whole profiles cannot be fitted with the Solomon–Bloembergen–Morgan (SBM) model due to the presence of zero-field splitting (ZFS), which affects the energy of the electron spin states.<sup>62,63</sup> The

**Figure 5.**  $^1\text{H}$  relaxivity profiles of GdDOTA-conjugated ANSII at 15, 25, and 37 °C. Solid lines are the best-fit profiles obtained with the Florence NMRD program, and dashed lines are calculated with the SBM model.

SBM model can however be used to reproduce the high-field regions of the profiles, when ZFS can be neglected because much smaller than the Zeeman energy. In the fit, outer-sphere contributions were also considered with typical values for the distance of closest approach and the diffusion coefficients.<sup>64</sup> The fit of the high-field region (proton Larmor frequencies larger than 5 MHz) shows that reorientation times  $\tau_i$  of the order of nanoseconds are needed to reproduce the profiles and their temperature dependence. These times are 1 order of magnitude smaller than the tumbling times of the tetrameric protein ( $\tau_R$ , see above), which implies that the dipole–dipole interactions between the unpaired electrons of the gadolinium(III) ions and the water protons are completely averaged out by internal dynamics.

The profiles were thus fitted using the modified Florence NMRD program,<sup>63,65,66</sup> which can reproduce the effects of the ZFS both in the electron and the nuclear relaxation rates, in the Redfield and slow rotation limits.<sup>67</sup> The slow rotation limit implies that reorientation is much slower than electron relaxation (determined from the parameters  $\Delta_t$  and  $\tau_v$  according to the pseudorotation model<sup>68</sup>). Contributions from even faster motions (with correlation time  $\tau_1$ ) were included through a Lipari–Szabo model-free approach<sup>11,69</sup> so as to further improve the quality of the fit. The best-fit parameters are reported in Table 2, and the corresponding profiles are

**Table 2. Best-Fit Parameters of the  $^1\text{H}$  Relaxivity Profiles of GdDOTA-Conjugated ANSII**

	15 °C	25 °C	37 °C	
$r^a$		3.05		Å
$q^a$		1		
$\Delta_t$		0.0095		$\text{cm}^{-1}$
$\tau_v$	$16 \times 10^{-12}$	$15 \times 10^{-12}$	$14 \times 10^{-12}$	s
$\tau_i$	$3.8 \times 10^{-9}$	$3.6 \times 10^{-9}$	$3.4 \times 10^{-9}$	s
$\tau_M$	$5.5 \times 10^{-7}$	$3.6 \times 10^{-7}$	$2.3 \times 10^{-7}$	s
$S^2$		0.71		
$\tau_1$	$1.7 \times 10^{-10}$	$1.2 \times 10^{-10}$	$0.8 \times 10^{-10}$	s
ZFS		0.03		$\text{cm}^{-1}$
$\theta$	35	47	55	degrees

<sup>a</sup>Fixed values. The outer-sphere parameters  $d$  (distance of closest approach) and  $D$  (diffusion coefficient) were fixed to  $3.6 \text{ Å}$  and to  $1.8 \times 10^{-9}$ ,  $2.3 \times 10^{-9}$ , and  $3.0 \times 10^{-9} \text{ m}^2 \text{ s}^{-1}$  at 15, 25, and 37 °C, respectively.



shown in Figure 5 as solid lines. The dashed lines in Figure 5 show the relaxivity profiles calculated with the same parameters and using the SBM model.

The best-fit profiles were obtained by allowing the angle  $\theta$  between the  $z$  axis of the ZFS tensor and the line passing through the positions of the gadolinium ion and the coordinated water molecule to change with changing temperature. The quality of the fit gets worse if  $\theta$  is constrained to be the same at all temperatures (unless the squared order parameter  $S^2$ ,  $\tau_{\text{M}}$ , and  $\tau_{\text{I}}$  are unrealistically allowed to increase with increasing temperature). Some inaccuracy in the calculated rates is expected because  $\tau_{\text{I}}$  and the electron relaxation time are of the same order of magnitude for frequencies smaller than 10 MHz, and therefore the slow rotation treatment is only approximate (more general approaches than the modified Florence NMRD program have been developed<sup>70–72</sup> for a more accurate treatment of these cases). This is however not preventing the accuracy of all other parameters, which are mainly determined from the relaxivity data at high fields, when ZFS is negligible and the SBM model holds.

In the fit, a single conformational state was assumed to be present. However, the variability of the angle  $\theta$  with temperature may also suggest the occurrence of multiple states, with a temperature-dependent equilibrium. At low temperatures, the gadolinium chelate may in fact interact to some extent with protein residues, whereas at higher temperatures, the increased mobility of the tag can favor more free and extended conformations.

The fit indicates an optimal reorientation time of few nanoseconds, and a lifetime of the coordinated water molecule of 0.2–0.5  $\mu\text{s}$ , i.e., about double with respect to the values observed for the free chelates in water.<sup>73,74</sup> A marked increase in the lifetime of the coordinated water molecule is often observed for gadolinium chelates conjugated to other proteins and macromolecular substrates. This increase is usually ascribed to the formation of hydrogen bonds involving the coordinated water itself and/or between the carboxylic groups of the ligand and amino acid side chains on the surface of the protein, which result in a significant release of the electric charge on the complex that, in turn, yields slower dissociation kinetics.<sup>75</sup> Figure 6 shows the largest enhancement in relaxivity, which can be achieved for an optimal lifetime of the

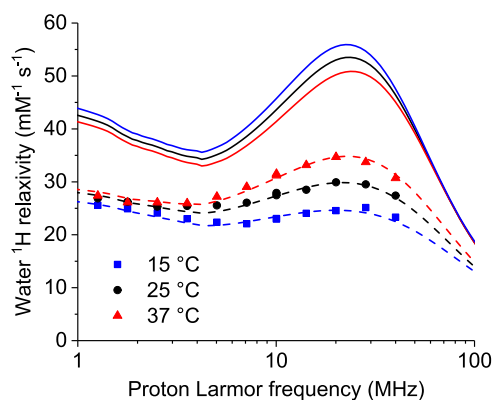


**Figure 6.**  $^1\text{H}$  relaxivity profiles calculated for optimized water exchange ( $\tau_{\text{M}} \approx 2\text{--}3 \times 10^{-8}$  s) and all other parameters equal to the values reported in Table 2 (solid lines). The experimental data for GdDOTA-conjugated ANSII are also reported.

coordinated water molecule of 20–30 ns. The profiles show that, for an optimized water exchange, at 1.5 T (ca. 60 MHz proton Larmor frequency), the relaxivity could increase from 25 to 34  $\text{s}^{-1} \text{mM}^{-1}$ . An even larger enhancement can be obtained at lower fields. An increase in the reorientation time, on the contrary, would produce a decrease in water relaxivity for fields higher than 1 T.

## CONCLUSIONS

The relaxometric profiles of the Gd-labeled ANSII indicate a relaxivity at about 1 T more than 5 times higher than that of clinically used contrast agents and quite high for a gadolinium-labeled protein. The analysis of the profiles sheds light on the origin of the observed relaxivity enhancement. The main contribution arises from the increased reorientational correlation time, amounting to few nanoseconds, i.e., only 1 order of magnitude larger than that of the unbound paramagnetic complex, but optimal for high-field MRI (1.5 T). Conversely, the observed slow exchange regime of the coordinated water molecules limits the relaxivity enhancement. It has been hypothesized that slow exchange arises from a pattern of hydrogen bonds involving the coordinated water itself, the carboxylic groups, and the amino acids at the protein surface. This view is supported by the short length of the linker connecting the paramagnetic core to the protein residues. We can speculate that the use of a longer linker may on the other hand decrease the reorientation time, leading to a decrease in relaxivity. A more interesting solution could be the use of a different gadolinium chelate, characterized by a faster exchange of the coordinated water, as, for instance, some DO3A derivatives,<sup>19</sup> which are sufficiently stable and inert for biological use.<sup>76</sup> The tetrameric assembly of the protein and the high relaxivity of the gadolinium chelates are key factors that make Gd(III)-labeled asparaginase an interesting model to develop new theranostic agents.

## EXPERIMENTAL PROCEDURES

**Protein Expression and Purification.** ANSII was expressed and purified in both nonlabeled and  $^{15}\text{N}$ -labeled forms, following the published protocol for ANSII production and purification.<sup>77</sup>

**Conjugation Reaction.** DOTA-NHS-ester solution was prepared by dissolving the reagent in a volume of dry DMF so that the percentage of organic solvent in the final 12 mL reaction volume was less than 1%. An excess of DOTA-NHS-ester (15 times the monomer concentration) with respect to a 0.152  $\text{mmol dm}^{-3}$  protein solution was employed for the conjugation. The reaction occurred overnight in 150  $\text{mmol dm}^{-3}$  phosphate buffer, pH 7.5, at room temperature.

A desalting column (Hi prep 26/10) was performed to eliminate the unreacted DOTA-NHS-ester and to change the buffer to 50  $\text{mmol dm}^{-3}$  MES–NaOH 100  $\text{mmol dm}^{-3}$  NaCl, pH 6.5.

**Chelation Reaction.** A 10  $\text{mmol dm}^{-3}$  solution of  $\text{GdCl}_3$  was added to the conjugated protein solution, to have a concentration of gadolinium(III) equal to 80% of the estimated DOTA-NHS-ester bound to the protein. The solution was incubated at 309 K and under stirring for 3 days overall.

Size exclusion chromatography using a HiLoad 16/60 Superdex 75 pg column was performed to remove the nonreacted gadolinium(III) ions.

**ICP-OES.** Inductively coupled plasma coupled with optical emission spectrometry was employed to determine gadolinium(III) concentration into the conjugated ANSII-DOTA sample.

**ESI MS Spectrometry.** The ESI MS investigations were performed using a TripleTOF 5600+ high-resolution mass spectrometer (Sciex, Framingham, MA), equipped with a DuoSpray interface operating with an ESI probe. All of the ESI mass spectra were acquired through direct infusion at 7  $\mu\text{L min}^{-1}$  flow rate.

The ESI source parameters optimized for the protein are the following:

Positive polarity, ionspray voltage floating (ISFV) 5500 V, temperature (TEM) 25  $^{\circ}\text{C}$ , ion source gas 1 (GS1) 25 L  $\text{min}^{-1}$ ; ion source gas 2 (GS2) 0 L  $\text{min}^{-1}$ ; curtain gas (CUR) 20 L  $\text{min}^{-1}$ , collision energy (CE) 10 V; declustering potential (DP) 30 V, acquisition range 500–3400  $m/z$ .

For acquisition, Analyst TF software 1.7.1 (Sciex) was used and deconvoluted spectra were obtained using the Bio Tool Kit micro-application v.2.2 embedded in PeakView software v.2.2 (Sciex).

Both samples were diluted to a final protein concentration of  $10^{-6}$  M using LC-MS water, pH 5.5, and the 0.5% v/v of formic acid was added just before the infusion in the mass spectrometer to enhance the ionization process.

The percentages of free ANSII and of its conjugates in the final sample has been calculated according to the relative intensity of each MS peak.

**$^1\text{H}$  NMRD.** Nuclear magnetic relaxation dispersion (NMRD) profiles were acquired with a fast-field-cycling Stellar relaxometer. They provided the field dependence of the longitudinal relaxation rate of water protons in samples with ANSII-DOTA solutions, from 0.01 to 40 MHz proton Larmor frequency.<sup>57</sup>

## ■ ASSOCIATED CONTENT

### SI Supporting Information

The Supporting Information is available free of charge at <https://pubs.acs.org/doi/10.1021/acs.bioconjchem.2c00506>.

Percentages of free and conjugated ANSII (Figure S1) and pKa and buried surface of amines of ANSII (Table S1) (PDF)

## ■ AUTHOR INFORMATION

### Corresponding Author

**Giacomo Parigi** – Magnetic Resonance Center (CERM), University of Florence, Sesto Fiorentino 50019, Italy; Department of Chemistry “Ugo Schiff”, University of Florence, Sesto Fiorentino 50019, Italy; Consorzio Interuniversitario Risonanze Magnetiche Metallo Proteine (CIRMMMP), Sesto Fiorentino 50019, Italy; [orcid.org/0000-0002-1989-4644](https://orcid.org/0000-0002-1989-4644); Email: [parigi@cerm.unifi.it](mailto:parigi@cerm.unifi.it)

### Authors

**Giulia Licciardi** – Magnetic Resonance Center (CERM), University of Florence, Sesto Fiorentino 50019, Italy; Department of Chemistry “Ugo Schiff”, University of Florence, Sesto Fiorentino 50019, Italy; Consorzio Interuniversitario Risonanze Magnetiche Metallo Proteine (CIRMMMP), Sesto Fiorentino 50019, Italy

**Domenico Rizzo** – Magnetic Resonance Center (CERM), University of Florence, Sesto Fiorentino 50019, Italy;

Department of Chemistry “Ugo Schiff”, University of Florence, Sesto Fiorentino 50019, Italy; Consorzio Interuniversitario Risonanze Magnetiche Metallo Proteine (CIRMMMP), Sesto Fiorentino 50019, Italy

**Maria Salobehaj** – Magnetic Resonance Center (CERM), University of Florence, Sesto Fiorentino 50019, Italy; Department of Chemistry “Ugo Schiff”, University of Florence, Sesto Fiorentino 50019, Italy; Consorzio Interuniversitario Risonanze Magnetiche Metallo Proteine (CIRMMMP), Sesto Fiorentino 50019, Italy

**Lara Massai** – Department of Chemistry “Ugo Schiff”, University of Florence, Sesto Fiorentino 50019, Italy

**Andrea Geri** – Department of Chemistry “Ugo Schiff”, University of Florence, Sesto Fiorentino 50019, Italy

**Luigi Messori** – Department of Chemistry “Ugo Schiff”, University of Florence, Sesto Fiorentino 50019, Italy; [orcid.org/0000-0002-9490-8014](https://orcid.org/0000-0002-9490-8014)

**Enrico Ravera** – Magnetic Resonance Center (CERM), University of Florence, Sesto Fiorentino 50019, Italy; Department of Chemistry “Ugo Schiff”, University of Florence, Sesto Fiorentino 50019, Italy; Consorzio Interuniversitario Risonanze Magnetiche Metallo Proteine (CIRMMMP), Sesto Fiorentino 50019, Italy; [orcid.org/0000-0001-7708-9208](https://orcid.org/0000-0001-7708-9208)

**Marco Fragai** – Magnetic Resonance Center (CERM), University of Florence, Sesto Fiorentino 50019, Italy; Department of Chemistry “Ugo Schiff”, University of Florence, Sesto Fiorentino 50019, Italy; Consorzio Interuniversitario Risonanze Magnetiche Metallo Proteine (CIRMMMP), Sesto Fiorentino 50019, Italy; [orcid.org/0000-0002-8440-1690](https://orcid.org/0000-0002-8440-1690)

Complete contact information is available at:

<https://pubs.acs.org/10.1021/acs.bioconjchem.2c00506>

## Notes

The authors declare no competing financial interest.

## ■ ACKNOWLEDGMENTS

The authors acknowledge the Fondazione Cassa di Risparmio di Firenze, the PRIN 2017A2KEPL project “Rationally designed nanogels embedding paramagnetic ions as MRI probes”, and the European Commission through H2020 FET-Open project HIRES-MULTIDYN (grant agreement no. 899683) for the financial support. They also acknowledge the support and the use of resources of Instruct-ERIC, a landmark ESFRI project, and specifically the CERM/CIRMMMP Italy center.

## ■ REFERENCES

- (1) Wahsner, J.; Gale, E. M.; Rodríguez-Rodríguez, A.; Caravan, P. Chemistry of MRI Contrast Agents: Current Challenges and New Frontiers. *Chem. Rev.* **2019**, *119*, 957–1057.
- (2) Gianolio, E.; Bardini, P.; Arena, F.; Stefania, R.; Di Gregorio, E.; Iani, R.; Aime, S. Gadolinium Retention in the Rat Brain: Assessment of the Amounts of Insoluble Gadolinium-Containing Species and Intact Gadolinium Complexes after Repeated Administration of Gadolinium-Based Contrast Agents. *Radiology* **2017**, *285*, 839–849.
- (3) McDonald, R. J.; McDonald, J. S.; Kallmes, D. F.; Jentoft, M. E.; Murray, D. L.; Thielen, K. R.; Williamson, E. E.; Eckel, L. J. Intracranial Gadolinium Deposition after Contrast-Enhanced MR Imaging. *Radiology* **2015**, *275*, 772–782.
- (4) Idée, J.-M.; Port, M.; Robic, C.; Medina, C.; Sabatou, M.; Corot, C. Role of Thermodynamic and Kinetic Parameters in Gadolinium Chelate Stability. *J. Magn. Reson. Imaging* **2009**, *30*, 1249–1258.

- (5) Di Gregorio, E.; Gianolio, E.; Stefania, R.; Barutello, G.; Digilio, G.; Aime, S. On the Fate of MRI Gd-Based Contrast Agents in Cells. Evidence for Extensive Degradation of Linear Complexes upon Endosomal Internalization. *Anal. Chem.* **2013**, *85*, 5627–5631.
- (6) Marckmann, P.; Skov, L.; Rossen, K.; Dupont, A.; Damholt, M. B.; Heaf, J. G.; Thomsen, H. S. Nephrogenic Systemic Fibrosis: Suspected Causative Role of Gadodiamide Used for Contrast-Enhanced Magnetic Resonance Imaging. *J. Am. Soc. Nephrol.* **2006**, *17*, 2359–2362.
- (7) Uzal-Varela, R.; Rodríguez-Rodríguez, A.; Martínez-Calvo, M.; Carniato, F.; Lalli, D.; Esteban-Gómez, D.; Brandariz, I.; Pérez-Lourido, P.; Botta, M.; Platas-Iglesias, C. Mn<sup>2+</sup> Complexes Containing Sulfonamide Groups with PH-Responsive Relaxivity. *Inorg. Chem.* **2020**, *59*, 14306–14317.
- (8) Rizzo, D.; Ravera, E.; Fragai, M.; Parigi, G.; Luchinat, C. Origin of the MRI Contrast in Natural and Hydrogel Formulation of Pineapple Juice. *Bioinorg. Chem. Appl.* **2021**, *2021*, 1–12.
- (9) Licciardi, G.; Rizzo, D.; Ravera, E.; Fragai, M.; Parigi, G.; Luchinat, C. Not Only Manganese, but Fruit Component Effects Dictate the Efficiency of Fruit Juice as an Oral Magnetic Resonance Imaging Contrast Agent. *NMR Biomed.* **2022**, *35*, No. e4623.
- (10) Wu, Y.; Zhou, I. Y.; Igarashi, T.; Longo, D. L.; Aime, S.; Sun, P. Z. A Generalized Ratiometric Chemical Exchange Saturation Transfer (CEST) MRI Approach for Mapping Renal PH Using Iopamidol. *Magn. Reson. Med.* **2018**, *79*, 1553–1558.
- (11) Caravan, P.; Cloutier, N. J.; McDermid, S. A.; Ellison, J. J.; Chasse, J. M.; Lauffer, R. B.; Luchinat, C.; McMurry, T. J.; Parigi, G.; Spiller, M. Albumin Binding, Relaxivity and Water Exchange Kinetics of the Diastereoisomers of MS-325 a Gadolinium(III) Based Magnetic Resonance Angiography Contrast Agent. *Inorg. Chem.* **2007**, *46*, 6632–6639.
- (12) Anelli, P. L.; Bertini, I.; Fragai, M.; Lattuada, L.; Luchinat, C.; Parigi, G. Sulfonamide-Functionalized Gadolinium DTPA Complexes as Possible Contrast Agents for MRI: A Relaxometric Investigation. *Eur. J. Inorg. Chem.* **2000**, *2000*, 625–630.
- (13) Li, H.; Parigi, G.; Luchinat, C.; Meade, T. J. Bimodal Fluorescence-Magnetic Resonance Contrast Agent for Apoptosis Imaging. *J. Am. Chem. Soc.* **2019**, *141*, 6224–6233.
- (14) Carniato, F.; Tei, L.; Botta, M.; Ravera, E.; Fragai, M.; Parigi, G.; Luchinat, C. <sup>1</sup>H NMR Relaxometric Study of Chitosan-Based Nanogels Containing Mono- and Bis-Hydrated Gd(III) Chelates: Clues for MRI Probes of Improved Sensitivity. *ACS Appl. Bio Mater.* **2020**, *3*, 9065–9072.
- (15) Fragai, M.; Ravera, E.; Tedoldi, F.; Luchinat, C.; Parigi, G. Relaxivity of Gd-Based MRI Contrast Agents in Crosslinked Hyaluronic Acid as a Model for Tissues. *ChemPhysChem* **2019**, *20*, 2204–2209.
- (16) Courant, T.; Roullin, V. G.; Cadiou, C.; Callewaert, M.; Andry, M. C.; Portefaix, C.; Hoeffel, C.; de Goltstein, M. C.; Port, M.; Laurent, S.; Elst, L. V.; Muller, R.; Molinari, M.; Chuburu, F. Hydrogels Incorporating GdDOTA: Towards Highly Efficient Dual T1/T2 MRI Contrast Agents. *Angew. Chem., Int. Ed.* **2012**, *51*, 9119–9122.
- (17) Yon, M.; Gineste, S.; Parigi, G.; Lonetti, B.; Gibot, L.; Talham, D. R.; Marty, J.-D.; Mingotaud, C. Hybrid Polymeric Nanostructures Stabilized by Zirconium and Gadolinium Ions for Use as Magnetic Resonance Imaging Contrast Agents. *ACS Appl. Nano Mater.* **2021**, *4*, 4974–4982.
- (18) Aime, S.; Frullano, L.; Geninatti Crich, S. Compartmentalization of a Gadolinium Complex in the Apoferritin Cavity: A Route To Obtain High Relaxivity Contrast Agents for Magnetic Resonance Imaging. *Angew. Chem., Int. Ed.* **2002**, *41*, 1017–1019.
- (19) Rotz, M. W.; Culver, K. S. B.; Parigi, G.; MacRenaris, K. W.; Luchinat, C.; Odom, T. W.; Meade, T. J. High Relaxivity Gd(III)–DNA Gold Nanostars: Investigation of Shape Effects on Proton Relaxation. *ACS Nano* **2015**, *9*, 3385–3396.
- (20) Carniato, F.; Tei, L.; Botta, M. Gd-Based Mesoporous Silica Nanoparticles as MRI Probes. *Eur. J. Inorg. Chem.* **2018**, *2018*, 4936–4954.
- (21) Carniato, F.; Tei, L.; Martinelli, J.; Botta, M. Relaxivity Enhancement of Ditopic Bishydrated Gadolinium(III) Complexes Conjugated to Mesoporous Silica Nanoparticles. *Eur. J. Inorg. Chem.* **2018**, *2018*, 2363–2368.
- (22) Tei, L.; Gugliotta, G.; Gambino, G.; Fekete, M.; Botta, M. Developing High Field MRI Contrast Agents by Tuning the Rotational Dynamics: Bisqua GdAAZTA-Based Dendrimers. *Isr. J. Chem.* **2017**, *57*, 887–895.
- (23) Alhaique, F.; Bertini, I.; Fragai, M.; Carafa, M.; Luchinat, C.; Parigi, G. Solvent <sup>1</sup>H NMRD Study of Biotinylated Paramagnetic Liposomes Containing Gd-Bis-SDA-DTPA or Gd-DMPE-DTPA. *Inorg. Chim. Acta* **2002**, *331*, 151–157.
- (24) Datta, A.; Hooker, J. M.; Botta, M.; Francis, M. B.; Aime, S.; Raymond, K. N. High Relaxivity Gadolinium Hydroxypyridonate–Viral Capsid Conjugates: Nanosized MRI Contrast Agents I. *J. Am. Chem. Soc.* **2008**, *130*, 2546–2552.
- (25) Mastarone, D. J.; Harrison, V. S. R.; Eckermann, A. L.; Parigi, G.; Luchinat, C.; Meade, T. J. A Modular System for the Synthesis of Multiplexed Magnetic Resonance Probes. *J. Am. Chem. Soc.* **2011**, *133*, 5329–5337.
- (26) Caravan, P.; Farrar, C. T.; Frullano, L.; Uppal, R. Influence of Molecular Parameters and Increasing Magnetic Field Strength on Relaxivity of Gadolinium- and Manganese-Based T1 Contrast Agents. *Contrast Media Mol. Imaging* **2009**, *4*, 89–100.
- (27) Matsumoto, Y.; Jasanoff, A. Metalloprotein-Based MRI Probes. *FEBS Lett.* **2013**, *587*, 1021–1029.
- (28) Yang, J. J.; Yang, J.; Wei, L.; Zurkiya, O.; Yang, W.; Li, S.; Zou, J.; Zhou, Y.; Maniccia, A. L. W.; Mao, H.; Zhao, F.; Malchow, R.; Zhao, S.; Johnson, J.; Hu, X.; Krogstad, E.; Liu, Z.-R. Rational Design of Protein-Based MRI Contrast Agents. *J. Am. Chem. Soc.* **2008**, *130*, 9260–9267.
- (29) Xue, S.; Qiao, J.; Pu, F.; Cameron, M.; Yang, J. J. Design of a Novel Class of Protein-Based Magnetic Resonance Imaging Contrast Agents for the Molecular Imaging of Cancer Biomarkers. *Wiley Interdiscip. Rev.: Nanomed. Nanobiotechnol.* **2013**, *5*, 163–179.
- (30) Caravan, P.; Greenwood, J. M.; Welch, J. T.; Franklin, S. J. Gadolinium-Binding Helix–Turn–Helix Peptides: DNA-Dependent MRI Contrast Agents. *Chem. Commun.* **2003**, 2574–2575.
- (31) Daughtry, K. D.; Martin, L. J.; Sarraju, A.; Imperiali, B.; Allen, K. N. Tailoring Encodable Lanthanide-Binding Tags as MRI Contrast Agents. *ChemBioChem* **2012**, *13*, 2567–2574.
- (32) Grum, D.; Franke, S.; Kraff, O.; Heider, D.; Schramm, A.; Hoffmann, D.; Bayer, P. Design of a Modular Protein-Based MRI Contrast Agent for Targeted Application. *PLoS One* **2013**, *8*, No. e65346.
- (33) Xue, S.; Yang, H.; Qiao, J.; Pu, F.; Jiang, J.; Hubbard, K.; Hekmatyar, K.; Langley, J.; Salarian, M.; Long, R. C.; Bryant, R. G.; Hu, X. P.; Grossniklaus, H. E.; Liu, Z.-R.; Yang, J. J. Protein MRI Contrast Agent with Unprecedented Metal Selectivity and Sensitivity for Liver Cancer Imaging. *Proc. Natl. Acad. Sci. U.S.A.* **2015**, *112*, 6607–6612.
- (34) Lauffer, R. B.; Brady, T. J. Preparation and Water Relaxation Properties of Proteins Labeled with Paramagnetic Metal Chelates. *Magn. Reson. Imaging* **1985**, *3*, 11–16.
- (35) Frullano, L.; Caravan, P. Strategies for the Preparation of Bifunctional Gadolinium(III) Chelators. *Curr. Org. Synth.* **2011**, *8*, 535–565.
- (36) Karfeld, L. S.; Bull, S. R.; Davis, N. E.; Meade, T. J.; Barron, A. E. Use of a Genetically Engineered Protein for the Design of a Multivalent MRI Contrast Agent. *Bioconjugate Chem.* **2007**, *18*, 1697–1700.
- (37) Karfeld-Sulzer, L. S.; Waters, E. A.; Davis, N. E.; Meade, T. J.; Barron, A. E. Multivalent Protein Polymer MRI Contrast Agents: Controlling Relaxivity via Modulation of Amino Acid Sequence. *Biomacromolecules* **2010**, *11*, 1429–1436.
- (38) Spanoghe, M.; Lanens, D.; Dommissse, R.; Van der Linden, A.; Alderweirdt, F. Proton Relaxation Enhancement by Means of Serum Albumin and Poly-L-Lysine Labeled with DTPA-Gd<sup>3+</sup>: Relaxivities as



a Function of Molecular Weight and Conjugation Efficiency. *Magn. Reson. Imaging* **1992**, *10*, 913–917.

(39) Rebizak, R.; Schaefer, M.; Dellacherie, É. Polymeric Conjugates of Gd<sup>3+</sup>–Diethylenetriaminopentacetic Acid and Dextran. 2. Influence of Spacer Arm Length and Conjugate Molecular Mass on the Paramagnetic Properties and Some Biological Parameters. *Bioconjugate Chem.* **1998**, *9*, 94–99.

(40) Zhang, Z.; Greenfield, M. T.; Spiller, M.; McMurry, T. J.; Lauffer, R. B.; Caravan, P. Multilocus Binding Increases the Relaxivity of Protein-Bound MRI Contrast Agents. *Angew. Chem., Int. Ed.* **2005**, *44*, 6766–6769.

(41) Tircsó, G.; Tircsóné Benyó, E.; Garda, Z.; Singh, J.; Trokowski, R.; Brücher, E.; Sherry, A. D.; Tóth, É.; Kovács, Z. Comparison of the Equilibrium, Kinetic and Water Exchange Properties of Some Metal Ion-DOTA and DOTA-Bis(Amide) Complexes. *J. Inorg. Biochem.* **2020**, *206*, No. 111042.

(42) Geraldes, C. F. G. C.; Luchinat, C. Lanthanides as Shift and Relaxation Agents in Elucidating the Structure of Proteins and Nucleic Acids. *Met. Ions Biol. Syst.* **2003**, *40*, 513–588.

(43) Keizers, P. H. J.; Ubbink, M. Paramagnetic Tagging for Protein Structure and Dynamics Analysis. *Prog. Nucl. Magn. Reson. Spectrosc.* **2011**, *58*, 88–96.

(44) Nitsche, C.; Otting, G. Chapter 2: Intrinsic and Extrinsic Paramagnetic Probes. In *Paramagnetism in Experimental Biomolecular NMR*; Royal Society of Chemistry, 2018; pp 42–84 DOI: [10.1039/9781788013291-00042](https://doi.org/10.1039/9781788013291-00042).

(45) Thonon, D.; Jacques, V.; Desreux, J. F. A Gadolinium Triacetic Monoamide DOTA Derivative with a Methanethiosulfonate Anchor Group. Relaxivity Properties and Conjugation with Albumin and Thiolated Particles. *Contrast Media Mol. Imaging* **2007**, *2*, 24–34.

(46) Tóth, É.; Pubanz, D.; Vauthey, S.; Helm, L.; Merbach, A. E. The Role of Water Exchange in Attaining Maximum Relaxivities for Dendritic MRI Contrast Agents. *Chem. - Eur. J.* **1996**, *2*, 1607–1615.

(47) Swain, A. L.; Jaskólski, M.; Housset, D.; Rao, J. K.; Wlodawer, A. Crystal Structure of Escherichia Coli L-Asparaginase, an Enzyme Used in Cancer Therapy. *Proc. Natl. Acad. Sci. U.S.A.* **1993**, *90*, 1474–1478.

(48) Hill, J. M.; Roberts, J.; Loeb, E.; Khan, A.; MacLellan, A.; Hill, R. W. L-Asparaginase Therapy for Leukemia and Other Malignant Neoplasms. Remission in Human Leukemia. *JAMA* **1967**, *202*, 882–888.

(49) Heo, Y.-A.; Syed, Y. Y.; Keam, S. J. Pegaspargase: A Review in Acute Lymphoblastic Leukaemia. *Drugs* **2019**, *79*, 767–777.

(50) Cerofolini, L.; Giuntini, S.; Carlon, A.; Ravera, E.; Calderone, V.; Fragai, M.; Parigi, G.; Luchinat, C. Characterization of PEGylated Asparaginase: New Opportunities from NMR Analysis of Large PEGylated Therapeutics. *Chem. - Eur. J.* **2019**, *25*, 1984–1991.

(51) Rosen, C. B.; Francis, M. B. Targeting the N Terminus for Site-Selective Protein Modification. *Nat. Chem. Biol.* **2017**, *13*, 697–705.

(52) Jiang, H.; D'Agostino, G. D.; Cole, P. A.; Dempsey, D. R. Selective Protein N-Terminal Labeling with N-Hydroxysuccinimide Esters. *Methods Enzymol.* **2020**, *639*, 333–353.

(53) Rostkowski, M.; Olsson, M. H.; Søndergaard, C. R.; Jensen, J. H. Graphical Analysis of pH-Dependent Properties of Proteins Predicted Using PROPKA. *BMC Struct. Biol.* **2011**, *11*, No. 6.

(54) Cutiño-Avila, B.; Gil, D.; González-Bacero, J.; Mokarzel-Falcón, L.; Chavez, M.; Díaz, J.; del Monte-Martínez, A. In *Algorithm Development for Protein Ionizable Group's Reactivity on Covalent Immobilization*; Rational Design of Immobilized Derivatives, 2010. DOI: [10.13140/2.1.1755.7769](https://doi.org/10.13140/2.1.1755.7769).

(55) Massai, L.; Zoppi, C.; Cirri, D.; Pratesi, A.; Messori, L. Reactions of Medicinal Gold(III) Compounds With Proteins and Peptides Explored by Electrospray Ionization Mass Spectrometry and Complementary Biophysical Methods. *Front. Chem.* **2020**, *8*, No. 581648.

(56) Cirri, D.; Massai, L.; Giacomelli, C.; Trincavelli, M. L.; Guerri, A.; Gabbiani, C.; Messori, L.; Pratesi, A. Synthesis, Chemical Characterization, and Biological Evaluation of a Novel Auranoform

Derivative as an Anticancer Agent. *Dalton Trans.* **2022**, *51*, 13527–13539.

(57) Parigi, G.; Ravera, E.; Fragai, M.; Luchinat, C. Unveiling Protein Dynamics in Solution with Field-Cycling NMR Relaxometry. *Prog. Nucl. Magn. Reson. Spectrosc.* **2021**, *124–125*, 85–98.

(58) Bertini, I.; Fragai, M.; Luchinat, C.; Parigi, G. <sup>1</sup>H NMRD Profiles of Diamagnetic Proteins: A Model-Free Analysis. *Magn. Reson. Chem.* **2000**, *38*, 543–550.

(59) Halle, B.; Jhannesson, H.; Venu, K. Model-Free Analysis of Stretched Relaxation Dispersions. *J. Magn. Reson.* **1998**, *135*, 1–13.

(60) Ravera, E.; Parigi, G.; Mainz, A.; Religa, T.; Reif, B.; Luchinat, C. Experimental Determination of Microsecond Reorientation Correlation Times in Protein Solutions. *J. Phys. Chem. B* **2013**, *117*, 3548–3553.

(61) Aime, S.; Botta, M.; Fasano, M.; Terreno, E. Lanthanide(II) Chelates for NMR Biomedical Applications. *Chem. Soc. Rev.* **1998**, *27*, 19–29.

(62) Parigi, G.; Ravera, E.; Luchinat, C. Magnetic Susceptibility and Paramagnetism-Based NMR. *Prog. Nucl. Magn. Reson. Spectrosc.* **2019**, *114–115*, 211–236.

(63) Bertini, I.; Galas, O.; Luchinat, C.; Parigi, G. A Computer Program for the Calculation of Paramagnetic Enhancements of Nuclear Relaxation Rates in Slowly Rotating Systems. *J. Magn. Reson. A* **1995**, *113*, 151–158.

(64) Freed, J. H. Dynamic Effects of Pair Correlation Functions on Spin Relaxation by Translational Diffusion in Liquids. II. Finite Jumps and Independent T<sub>1</sub> Processes. *J. Chem. Phys.* **1978**, *68*, 4034–4037.

(65) Bertini, I.; Kowalewski, J.; Luchinat, C.; Nilsson, T.; Parigi, G. Nuclear Spin Relaxation in Paramagnetic Complexes of S = 1: Electron Spin Relaxation Effects. *J. Chem. Phys.* **1999**, *111*, 5795–5807.

(66) Kruk, D.; Nilsson, T.; Kowalewski, J. Nuclear Spin Relaxation in Paramagnetic Systems with Zero-Field Splitting and Arbitrary Electron Spin. *Phys. Chem. Chem. Phys.* **2001**, *3*, 4907–4917.

(67) Kowalewski, J.; Luchinat, C.; Nilsson, T.; Parigi, G. Nuclear Spin Relaxation in Paramagnetic Systems: Electron Spin Relaxation Effects under Near-Redfield Limit Conditions and Beyond. *J. Phys. Chem. A* **2002**, *106*, 7376–7382.

(68) Bloembergen, N.; Morgan, L. O. Proton Relaxation Times in Paramagnetic Solutions. Effects of Electron Spin Relaxation. *J. Chem. Phys.* **1961**, *34*, 842–850.

(69) Lipari, G.; Szabo, A. Model-Free Approach to the Interpretation of Nuclear Magnetic Resonance Relaxation in Macromolecules. 1. Theory and Range of Validity. *J. Am. Chem. Soc.* **1982**, *104*, 4546–4559.

(70) Fries, P. H. Computing Electronic Spin Relaxation for Gd<sup>3+</sup>-Based Contrast Agents – Practical Implementation. *Eur. J. Inorg. Chem.* **2012**, *2012*, 2156–2166.

(71) Kowalewski, J.; Kruk, D.; Parigi, G. NMR Relaxation in Solution of Paramagnetic Complexes: Recent Theoretical Progress for S > 1. *Adv. Inorg. Chem.* **2005**, *57*, 41–104.

(72) Belorizky, E.; Fries, P. H.; Helm, L.; Kowalewski, J.; Kruk, D.; Sharp, R. R.; Westlund, P.-O. Comparison of Different Methods for Calculating the Paramagnetic Relaxation Enhancement of Nuclear Spins as a Function of the Magnetic Field. *J. Chem. Phys.* **2008**, *128*, No. 052315.

(73) Powell, D. H.; Dhubhghaill, O. M. N.; Pubanz, D.; Helm, L.; Lebedev, Y. S.; Schlaepfer, W.; Merbach, A. E. Structural and Dynamic Parameters Obtained from <sup>17</sup>O NMR, EPR, and NMRD Studies of Monomeric and Dimeric Gd<sup>3+</sup> Complexes of Interest in Magnetic Resonance Imaging: An Integrated and Theoretically Self-Consistent Approach I. *J. Am. Chem. Soc.* **1996**, *118*, 9333–9346.

(74) Laurent, S.; Elst, L. V.; Muller, R. N. Comparative Study of the Physicochemical Properties of Six Clinical Low Molecular Weight Gadolinium Contrast Agents. *Contrast Media Mol. Imaging* **2006**, *1*, 128–137.

(75) Aime, S.; Castelli, D. D.; Crich, S. G.; Gianolio, E.; Terreno, E. Pushing the Sensitivity Envelope of Lanthanide-Based Magnetic



Resonance Imaging (MRI) Contrast Agents for Molecular Imaging Applications. *Acc. Chem. Res.* **2009**, *42*, 822–831.

(76) Takács, A.; Napolitano, R.; Purgel, M.; Bényei, A. C.; Zékány, L.; Brücher, E.; Tóth, I.; Baranyai, Z.; Aime, S. Solution Structures, Stabilities, Kinetics, and Dynamics of DO3A and DO3A–Sulphonamide Complexes. *Inorg. Chem.* **2014**, *53*, 2858–2872.

(77) Ravera, E.; Ciambellotti, S.; Cerofolini, L.; Martelli, T.; Kozyreva, T.; Bernacchioni, C.; Giuntini, S.; Fragai, M.; Turano, P.; Luchinat, C. Solid-State NMR of PEGylated Proteins. *Angew. Chem., Int. Ed.* **2016**, *55*, 2446–2449.

## Recommended by ACS

### Design Principles of Responsive Relaxometric $^{19}\text{F}$ Contrast Agents: Evaluation from the Point of View of Relaxation Theory and Experimental Data

Mariusz Zalewski, Tomasz Krawczyk, *et al.*

NOVEMBER 16, 2022  
INORGANIC CHEMISTRY

READ 

### Derivatives of GdAAZTA Conjugated to Amino Acids: A Multinuclear and Multifrequency NMR Study

Daniela Lalli, Mauro Botta, *et al.*

AUGUST 09, 2022  
INORGANIC CHEMISTRY

READ 

### Effect of Structural Fine-Tuning on Chelate Stability and Liver Uptake of Anionic MRI Contrast Agents

Ah Rum Baek, Yongmin Chang, *et al.*

APRIL 14, 2022  
JOURNAL OF MEDICINAL CHEMISTRY

READ 

### Physico-Chemical Characterization of a Highly Rigid Gd(III) Complex Formed with a Phenanthroline Derivative Ligand

Balázs Váradi, Ferenc K. Kálmán, *et al.*

AUGUST 16, 2022  
INORGANIC CHEMISTRY

READ 

Get More Suggestions >